

## Magnetic ordering in a weakly coupled Fe/V(001) superlattice

Till Burkert,<sup>1,\*</sup> Peter Svedlindh,<sup>2</sup> Gabriella Andersson,<sup>1</sup> and Björgvin Hjörvarsson<sup>1</sup>

<sup>1</sup>Department of Physics, Uppsala University, Box 530, 751 21 Uppsala, Sweden

<sup>2</sup>Department of Materials Science, Uppsala University, Box 534, 751 21 Uppsala, Sweden

(Received 15 August 2002; published 17 December 2002)

A large shift of the ordering temperature is observed in an Fe<sub>3</sub>/V<sub>13</sub>(001) superlattice upon altering the interlayer coupling  $J'$ . The modification of  $J'$  is accomplished by temporary alloying of the V spacer layers with hydrogen. A phase with short-range magnetic order is found in a wide temperature range between the paramagnetic phase and the onset of long-range order. It is interpreted as two-dimensional-XY behavior and is attributed to the absence of an in-plane magnetic anisotropy and the vanishing of the interlayer exchange coupling close to the ordering temperature.

DOI: 10.1103/PhysRevB.66.220402

PACS number(s): 75.70.Ak, 75.30.-m, 75.40.Cx, 75.40.-s

Magnetic phase transitions can be divided into universal classes according to the spatial dimensionality and the magnetic anisotropy of the system. Its spatial dimensionality is determined by the extent to which the critical fluctuations can propagate at the phase transition. The presence or absence of a phase transition to magnetic long-range order at a finite Curie or Néel temperature depends on which universality class a particular magnet belongs to.<sup>1</sup> In strictly two-dimensional (2D) magnets, the presence of a phase transition to conventional long-range order is crucially dependent on the magnetic anisotropy. It does exist in magnets with a uniaxial magnetic anisotropy (2D-Ising), but is prohibited—as described by the Mermin-Wagner theorem—in the case of planar (2D-XY) and isotropic (2D-Heisenberg) spin symmetry.<sup>2</sup> A Kosterlitz-Thouless phase transition, to a phase with so-called topological short-range order, occurs at a finite temperature in the 2D-XY model.<sup>3,4</sup> The Kosterlitz-Thouless phase comprises bound vortex-antivortex pairs that destroy the long-range magnetic order in infinite magnets. In real magnets, however, the finite size gives rise to a spontaneous magnetization.<sup>5</sup>

Experimental investigations of dimensionality aspects of magnetic phase transitions are often conducted on layered magnets, such as illustrated in Fig. 1. They consist of ultrathin magnetic films with an intralayer coupling  $J$  within the layers separated by nonmagnetic spacer layers. Adjacent magnetic layers are coupled via an interlayer coupling  $J' \ll J$  across the spacer. Virtually all layered systems are quasi-2D since an interlayer coupling always exists. Nevertheless, two-dimensional behavior can be expected for sufficiently weak interlayer coupling.<sup>6</sup> A transition to three-dimensional behavior occurs at a finite temperature if the in-plane correlations are sufficiently well developed.

Previous studies of dimensionality aspects of magnetic phase transitions were focused on layered transition-metal based compounds.<sup>7</sup> In the quasi-2D Heisenberg ferromagnet (C<sub>n</sub>H<sub>2n+1</sub>NH<sub>3</sub>)<sub>2</sub>CuCl<sub>4</sub> ( $n = 1, 2, 3, 10$ ), e.g., both the ratio  $J'/J$  as well as the magnetic anisotropy depend on the composition  $n$ .<sup>8,9</sup> This system shows a crossover from 2D to 3D behavior at  $T_C^+$  as well as spin-dimensionality crossovers due to the presence of small XY and Ising anisotropies. The usefulness of these “classical” systems is limited by structural imperfections that hinder the divergence of the critical fluc-

tuations at the phase transitions as well as the accessible range of the interlayer coupling. An alternative route is to utilize metallic magnetic samples which have a superior in-plane structural coherence. The strength of the interlayer coupling—which is of exchange-type in metallic samples—oscillates as a function of the spacer thickness  $d$  and decreases as  $1/d^2$ .<sup>10</sup> Thus, the influence of the interlayer coupling can be studied in a series of samples with different spacer thicknesses.

Fe/V(001) superlattices are examples of metallic heterostructures with a superior structural coherence and magnetic homogeneity.<sup>11,12</sup> Only recently magnetic-susceptibility measurements on an Fe<sub>2</sub>/V<sub>5</sub>(001) superlattice (the subscripts denote the number of monolayers in each period of the stack) have been reported.<sup>13</sup> The composition of this particular sample results in an in-plane magnetic anisotropy and a rather strong interlayer exchange coupling. From the 2D-Ising-like critical exponent that was observed at  $T_C^+$  a vanishing of the interlayer exchange coupling in the vicinity of  $T_C$  was inferred. The same behavior was observed in Ni/Cu/Co and Ni/Cu/Ni trilayers and seems to be a universal property of exchange-coupled metallic heterostructures.<sup>14</sup> Thus, two-dimensional behavior can be expected in metallic magnetic superlattices close to the ordering temperature.

The purpose of this communication is to address the question whether 2D-XY-like behavior can be observed in metallic ferromagnetic superlattices. The approach of temporary alloying taken here allows for the investigation of the magnetic order as a function of the interlayer coupling in a *single* sample, an Fe<sub>3</sub>/(VH<sub>x</sub>)<sub>13</sub>(001) superlattice. The interlayer coupling is modified by changing the hydrogen concentration<sup>26</sup>  $x \equiv \langle H/V \rangle$  in the V layers.<sup>15,16</sup> This type of superlattice has an isotropic easy-plane magnetization and

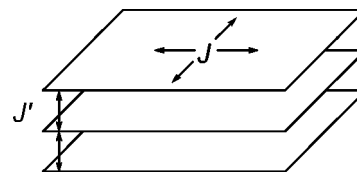


FIG. 1. Illustration of a layered magnet. The 2D magnetic layers have an intralayer coupling  $J$  within the layers. Adjacent layers are coupled by an interlayer coupling  $J' \ll J$ .

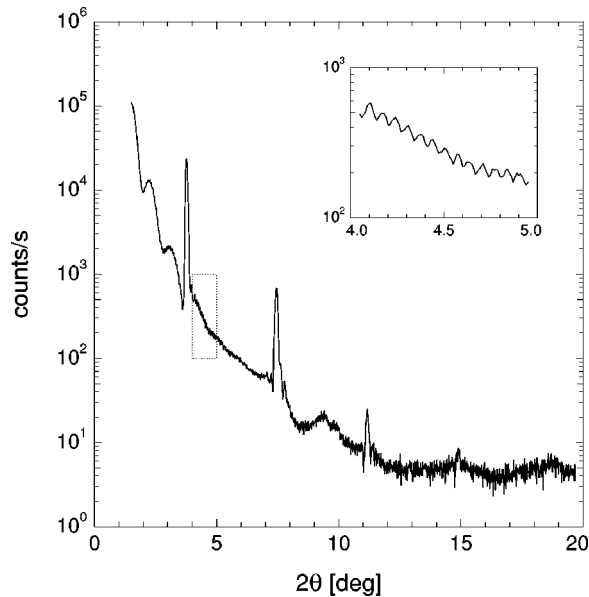


FIG. 2. X-ray reflectivity of the Pd/[V<sub>13</sub>/Fe<sub>3</sub>]<sub>50</sub>/MgO(001) superlattice. The inset shows the Kiessig fringes due to the well-defined total thickness of the superlattice.

should therefore exhibit characteristics of the XY model.<sup>17,18</sup> The magnetic ordering is studied by means of low-frequency susceptibility and magnetization measurements using the magneto-optic Kerr effect (MOKE).

The sample consists of 50 repetitions of Fe<sub>3</sub>/V<sub>13</sub> grown on MgO(001) by dc magnetron sputtering in UHV.<sup>11</sup> A 10-nm-thick Pd capping layer was applied to prevent deterioration of the sample and to facilitate hydrogen uptake. The x-ray reflectivity pattern shown in Fig. 2 demonstrates that the superlattice period of 2.39 nm and the total thickness of the stack are well defined. The thickness variation of the constituents is close to one monolayer, which is the limit for non phase-locked epitaxial growth. Thus, the sample is composed of large structurally correlated two-dimensional magnetic sheets. X-ray-diffraction measurements (not shown here) confirm a good crystalline quality. The full width at half maximum (FWHM) of the (002) rocking curve is 0.3°.

The MOKE susceptibility and magnetization measurements were performed in an ultrahigh vacuum based chamber specifically designed for the purpose of these measurements. The shielding of the earth's magnetic field is accomplished by a double mu-metal cover. A pair of Helmholtz coils inside the chamber allows very small and homogeneous excitation fields. For all susceptibility measurements reported here an excitation field of 0.013 mT at 70 Hz was used. Temperature scans were accomplished by heating the whole chamber at a rate of 0.1 K/min between 300 and 350 K. Such a low rate ensures that the sample is thermally equilibrated. The magnetization measurements were performed in remanence, aligning the magnetization with a magnetic-field pulse in either direction and taking the difference of the Kerr signal as a measure of the magnetization.

In Fig. 3 results for the magnetic susceptibility  $\chi = \chi' - i\chi''$  for the sample without hydrogen and at three different hydrogen pressures  $p_{H_2}$  are presented. The susceptibility of

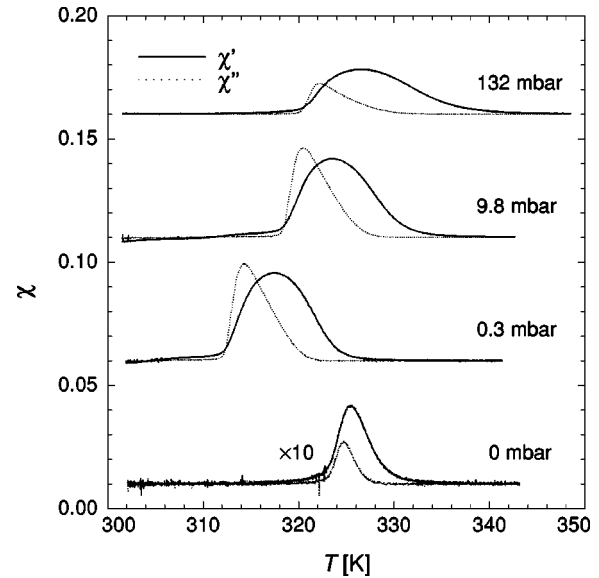


FIG. 3. Magnetic susceptibility at different hydrogen pressures. The signal of the sample containing no hydrogen has been enlarged for clarification. Note the excellent signal-to-noise ratio of the raw data.

the sample containing no hydrogen is more than one order of magnitude less than that of the hydrogenated samples. This is expected for the antiferromagnetically coupled Fe<sub>3</sub>/V<sub>13</sub>(001) superlattice.<sup>18</sup> The character of the coupling has been confirmed by MOKE hysteresis loops (not shown here). Hydrogen pressures as low as 0.2 mbar give rise to a sizable increase of the susceptibility signal and a shift of its maximum to lower temperatures. For the discussion of this behavior it is necessary to relate the measured susceptibility to the remanent magnetization  $M_r$  in order to draw conclusions on the magnetic order.

Figure 4 shows the magnetic susceptibility and the corresponding remanent magnetization at 557 mbar hydrogen pressure. The characteristic temperatures  $T_1$  and  $T_2$  mark the maxima in the susceptibility and the corresponding transitions that are discussed in the following. The peak at  $T_1$  is accompanied by an onset of a small remanent magnetization. Because of the large width of this peak (9 K FWHM), we define the appearance of hysteresis losses (a nonvanishing  $\chi''$ ) as a marker for this transition. At  $T_2$ , defined as the maximum of  $\chi'$ , a rapid increase of  $M_r$  is observed. The FWHM of this peak is only 1 K and of the size usually reported for high-quality magnetic superlattices and thin films.<sup>13,19</sup> The remanent magnetization increases further as the temperature is lowered. The “inverse” third peak in the susceptibility at approximately 305 K is phase shifted by 180° relative to the transitions at  $T_1$  and  $T_2$ . No change in the remanent magnetization is observed here. Its origin is so far unclear.

We interpret the slow increase of the remanent magnetization at  $T_1$  as a gradual transition from the paramagnetic phase (PM) to a phase with magnetic short-range order (SRO), and the rapid increase of  $M_r$  at  $T_2$  as the onset of magnetic long-range order (LRO). The existence of a quasi-2D phase with decoupled magnetic layers between  $T_1$

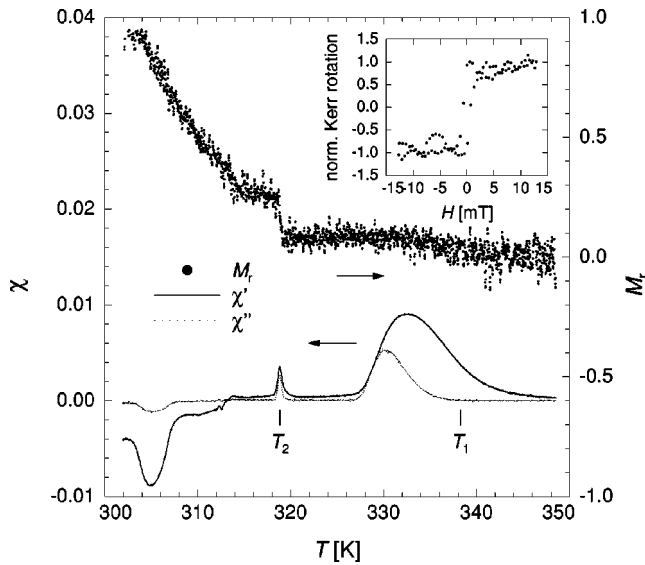


FIG. 4. Magnetic susceptibility (lower part) and remanent magnetization  $M_r$  (upper part) at  $p_{\text{H}_2} = 557$  mbar. The  $M_r$  raw data has been smoothed. The positions of the characteristic temperatures  $T_1$  and  $T_2$  are indicated. The inset shows a hysteresis loop at 300 K.

and  $T_2$  is in accordance with the vanishing of the interlayer exchange coupling at  $T_C^+$  in metallic heterostructures.<sup>13,14</sup> The different behavior reported here as compared to the 2D-Ising-like behavior observed in an  $\text{Fe}_2/\text{V}_5(001)$  superlattice with uniaxial magnetic anisotropy<sup>13</sup> is due to the absence of an in-plane anisotropy in the present sample. At  $T_2$  the interlayer exchange coupling is strong enough to couple the individual magnetic layers over the nonmagnetic spacer. It thereby induces a long-range order of the two-dimensional magnetic sheets. The inset in Fig. 4 shows a hysteresis loop recorded at 300 K that supports the interpretation of a long-range ordered phase in that temperature region. Hysteresis loops recorded at higher temperatures are less conclusive due to the bad signal-to-noise ratio and are not shown here. The stabilization of a spontaneous magnetization at  $T_2$  is either due to a dimensionality crossover from 2D to 3D, or due to the mere perturbation that  $J'$  constitutes.<sup>20</sup> We therefore conclude that 2D-XY-like behavior can indeed be observed in metallic ferromagnetic superlattices.

The shift of the susceptibility maximum to lower temperatures upon hydrogenation shown in Fig. 3 is attributed to a weakening of the interlayer exchange coupling. Whereas the  $p_{\text{H}_2} = 0$  mbar susceptibility maximum is due to a transition from the paramagnetic phase to a phase with antiferromagnetic long-range order, the transitions in the hydrogenated samples are to a state of short-range magnetic order (referred to as  $T_1$  in the previous discussion). The onset of a remanent magnetization at  $T_2$  for the data shown in Fig. 3 is outside the temperature range of the present experiments. The fact that a remanent magnetization is observed at larger hydrogen pressures is attributed to a change of sign of the interlayer coupling, leading to a ferromagnetic order below  $T_2$ , and has been observed previously.<sup>15,16</sup>

An analysis of the critical behavior at  $T_2$  revealed a power-law dependence of the susceptibility. Although a rea-

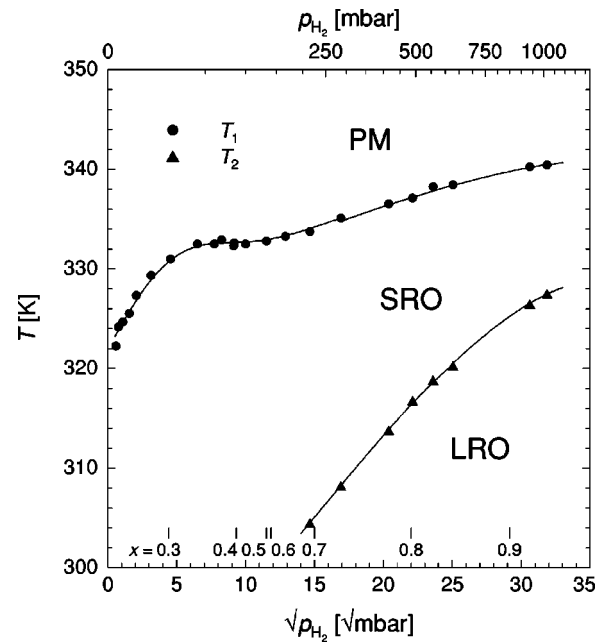


FIG. 5. Characteristic temperatures  $T_1$  and  $T_2$  as a function of hydrogen pressure. The hydrogen concentration  $x$  is indicated at the bottom of the plot. PM, SRO, and LRO denote the types of magnetic order in the hydrogenated sample.

sonable value was obtained for the critical exponent  $\gamma = 1.5 \pm 0.3$ , no conclusion could be reached about the universality class of this particular transition because of the ambiguity in defining the critical temperature. As for the peak at  $T_1$ , no attempt has been made to analyze its critical behavior because of its large FWHM.

Figure 5 shows the dependence of the characteristic temperatures  $T_1$  and  $T_2$  on hydrogen pressure. It constitutes a  $p_{\text{H}_2}$ - $T$  phase diagram of the different types of magnetic order discussed above. Note that only the hydrogenated sample is considered here. The antiferromagnetic ordering at  $p_{\text{H}_2} = 0$  is not included in the phase diagram. The hydrogen concentration  $x$  in the V layers was estimated from a solubility isotherm previously measured on an identical sample.<sup>21</sup> The increase of  $T_1$  with hydrogen concentration is in accordance with the enhanced Fe magnetic moment and the correspondingly increased  $T_C$  reported by Laberge *et al.*<sup>22</sup> Thus,  $T_1$  serves as a measure of the intralayer coupling. The plateau in  $T_1$  at  $x \approx 0.4$  is accompanied by a broadening of this peak (cf. Fig. 3) as well as a hysteresis in the susceptibility between raising and lowering the temperature (not shown here). It is attributed to an ordering phenomenon that has previously been observed in studies of the hydrogen uptake of  $\text{Fe}/\text{V}(001)$  superlattices.<sup>21</sup> The ordering gives rise to an inhomogeneous distribution of hydrogen atoms in the V host and causes a variation of the Fe magnetic moments and a distribution of transition temperatures. This interpretation is supported by the fact that the increased FWHM is of the same size as the change of  $T_1$  observed when varying the hydrogen concentration in the range covered by the present measurements.

The faster increase of  $T_2$  as compared to  $T_1$  (cf. Fig. 5) is

attributed to the strong dependence of  $J'$  on hydrogen concentration observed here and in Ref. 15. A shift of the susceptibility maximum as a function of the interlayer coupling has first been observed in asymmetric (the decoupled magnetic layers have different  $T_C$ ) exchange-coupled Co/Cu/Ni and Ni/Cu/Ni trilayers.<sup>23,24</sup> The present results are the direct observation of such a shift in a magnetically symmetric heterostructure. Bayreuther *et al.* studied the shift of  $T_C$  as a function of the interlayer coupling by magnetization measurements on a set of symmetric Ni/Au multilayers.<sup>25</sup> The approach of temporary alloying taken here removes the ambiguity related to thickness variations that can not be avoided if a series of samples is used.

In conclusion, two-dimensional XY-like behavior can be observed in metallic ferromagnetic superlattices. The conditions that have to be met are: a two-dimensional character

and a sufficiently large structural coherence of the magnetic layers, an easy-plane magnetic anisotropy, and a sufficiently weak interlayer exchange coupling. The encountered two-dimensional behavior supports the recent finding of a vanishing interlayer exchange coupling close to  $T_C$  in metallic heterostructures. Furthermore, we present a direct proof of a shift of the susceptibility maximum induced by the interlayer coupling in a magnetically symmetric heterostructure.

We gratefully acknowledge P. Blomqvist for the growth and structural characterization of the sample and S. Olsson for valuable discussion. This work was supported by the TMR network *Switchable Metal-hydride Films*, the Swedish Research Council, and the network *Fundamental Research and Applications of Magnetism* funded by the Swedish Foundation for Strategic Research.

\*Electronic address: till.burkert@fysik.uu.se

<sup>1</sup>L.J. de Jongh, in *Magnetic Properties of Layered Transition Metal Compounds* (Ref. 7), pp. 1–51.

<sup>2</sup>N.D. Mermin and H. Wagner, *Phys. Rev. Lett.* **17**, 1133 (1966).

<sup>3</sup>J.M. Kosterlitz and D.J. Thouless, *J. Phys. C* **6**, 1181 (1973).

<sup>4</sup>J.M. Kosterlitz, *J. Phys. C* **7**, 1046 (1974).

<sup>5</sup>S.T. Bramwell and P.C.W. Holdsworth, *J. Phys.: Condens. Matter* **5**, L53 (1993).

<sup>6</sup>J.M. Kosterlitz and M.A. Santos, *J. Phys. C* **11**, 2835 (1978).

<sup>7</sup>*Magnetic Properties of Layered Transition Metal Compounds*, edited by L.J. de Jongh, (Kluwer Academic, Dordrecht, 1990).

<sup>8</sup>L.J. de Jongh, *Physica B & C* **82**, 247 (1976).

<sup>9</sup>L.J. de Jongh and H.E. Stanley, *Phys. Rev. Lett.* **36**, 817 (1976).

<sup>10</sup>P. Bruno, *J. Phys.: Condens. Matter* **11**, 9403 (1999).

<sup>11</sup>P. Isberg, B. Hjörvarsson, R. Wäppling, E.B. Svedberg, and L. Hultman, *Vacuum* **48**, 483 (1997).

<sup>12</sup>A.N. Anisimov, W. Platow, P. Pouloupoulos, W. Wisny, M. Farle, K. Baberschke, P. Isberg, B. Hjörvarsson, and R. Wäppling, *J. Phys.: Condens. Matter* **9**, 10 581 (1997).

<sup>13</sup>C. Rüdt, P. Pouloupoulos, J. Lindner, A. Scherz, H. Wende, K. Baberschke, P. Blomqvist, and R. Wäppling, *Phys. Rev. B* **65**, 220404(R) (2002).

<sup>14</sup>J. Lindner, C. Rüdt, E. Kosubek, P. Pouloupoulos, K. Baberschke, P. Blomqvist, R. Wäppling, and D.L. Mills, *Phys. Rev. Lett.* **88**, 167206 (2002).

<sup>15</sup>D. Laberge, C. Sutter, H. Zabel, and B. Hjörvarsson, *J. Magn. Magn. Mater.* **192**, 238 (1999).

<sup>16</sup>B. Hjörvarsson, J.A. Dura, P. Isberg, T. Watanabe, T.J. Udovic, G. Andersson, and C.F. Majkrzak, *Phys. Rev. Lett.* **79**, 901 (1997).

<sup>17</sup>P. Pouloupoulos, P. Isberg, W. Platow, W. Wisny, M. Farle, B. Hjörvarsson, and K. Baberschke, *J. Magn. Magn. Mater.* **170**, 57 (1997).

<sup>18</sup>P. Granberg, P. Isberg, E.B. Svedberg, B. Hjörvarsson, P. Nordblad, and R. Wäppling, *J. Magn. Magn. Mater.* **186**, 154 (1998).

<sup>19</sup>F. Bensch, G. Garreau, R. Moosbühler, G. Bayreuther, and E. Beaurepaire, *J. Appl. Phys.* **89**, 7133 (2001).

<sup>20</sup>P.J. Jensen, K.H. Bennemann, P. Pouloupoulos, M. Farle, F. Wilhelm, and K. Baberschke, *Phys. Rev. B* **60**, R14994 (1999).

<sup>21</sup>S. Olsson, P. Blomqvist, and B. Hjörvarsson, *J. Phys.: Condens. Matter* **13**, 1685 (2001).

<sup>22</sup>D. Laberge, K. Westerholt, H. Zabel, and B. Hjörvarsson, *J. Magn. Magn. Mater.* **225**, 373 (2001).

<sup>23</sup>U. Bovensiepen, F. Wilhelm, P. Srivastava, P. Pouloupoulos, M. Farle, A. Ney, and K. Baberschke, *Phys. Rev. Lett.* **81**, 2368 (1998).

<sup>24</sup>P. Pouloupoulos, U. Bovensiepen, M. Farle, and K. Baberschke, *J. Magn. Magn. Mater.* **212**, 17 (2000).

<sup>25</sup>G. Bayreuther, F. Bensch, and V. Kottler, *J. Appl. Phys.* **79**, 4509 (1996).

<sup>26</sup>All concentrations quoted here are *interior*. For the present sample, two monolayers are depleted of hydrogen close to each V-Fe interface (Ref. 21).